

LIMITS ON NEW LEPTON PAIRS (L^- , L^0)
WITH ARBITRARY NEUTRINO MASS

D.P. Stoker, ^{α} M.L. Perl, ^{β} G. Abrams, ^{γ} A.R. Baden, ^{$\gamma,(a)$} T. Barklow, ^{β}
B.A. Barnett, ^{α} A.M. Boyarski, ^{β} J. Boyer, ^{γ} P.R. Burchat, ^{$\beta,(b)$} F. Butler, ^{γ}
J.M. Dorfan, ^{β} G.J. Feldman, ^{β} G. Gidal, ^{γ} G. Hanson, ^{β} B.D. Harral, ^{α}
K. Hayes, ^{β} D. Herrup, ^{$\gamma,(c)$} J.E. Hylen, ^{α} W.R. Innes, ^{β} J.A. Jaros, ^{β}
J.A. Kadyk, ^{γ} D. Karlen, ^{$\beta,(d)$} S.R. Klein, ^{$\beta,(e)$} A.J. Lankford, ^{β} B.W. LeClaire, ^{$\beta,(f)$}
M. Levi, ^{$\beta,(g)$} V. Lüth, ^{β} J.A.J. Matthews, ^{α} R.A. Ong, ^{$\beta,(h)$} K. Riles, ^{β}
P.C. Rowson, ^{$\gamma,(i)$} and D.R. Wood ^{$\gamma,(j)$}

^{α} *Johns Hopkins University, Baltimore, Maryland 21218*

^{β} *Stanford Linear Accelerator Center, Stanford University, Stanford, California 94309*

^{γ} *Lawrence Berkeley Laboratory and Department of Physics, University of California,
Berkeley, California 94720*

Abstract

We have searched 205 pb^{-1} of $\sqrt{s} = 29 \text{ GeV}$ data from the MARK II detector at PEP for events which may signify the existence of a new lepton pair (L^- , L^0) where the L^0 may be massive, but does not exceed the L^- mass. Three event signatures for L^+L^- decay are examined: (i) $e^\pm\mu^\mp$, (ii) $(e \text{ or } \mu)^\pm(\pi^\mp + \leq 4\gamma)$, and (iii) $(e \text{ or } \mu)^\pm(\geq 3\pi^\pm + \geq 0\gamma)^\mp$. The numbers of signature events are found to be in good agreement with Monte Carlo simulations of known background sources. The ranges of L^- and L^0 masses for which new lepton pairs are excluded are obtained using a probability ratio method to compare the number of observed signature events to the expected background, and to the expected background plus Monte Carlo predictions of (L^- , L^0) signals.

Submitted to Physical Review D

* This work was supported in part by National Science Foundation grants PHY-8404562 and PHY-8701610 (Johns Hopkins), and Department of Energy contracts DE-AC03-76SF00515 (SLAC) and DE-AC03-76SF00098 (LBL).

(a) Present address: Harvard University, Cambridge, MA 02138.

(b) Present address: University of California, Santa Cruz, CA 95064.

(c) Present address: Fermi National Laboratory, Batavia, IL 60510.

(d) Present address: Carleton University, Ottawa, Canada K1S 5B6.

(e) Present address: Boston University, Boston, MA 02215.

(f) Present address: University of Wisconsin, Madison, WI 53706.

(g) Present address: Lawrence Berkeley Laboratory, Berkeley, CA 94720.

(h) Present address: University of Chicago, Chicago, IL 60637.

(i) Present address: Columbia University, New York, NY 10027.

(j) Present address: CERN, CH-1211, Genève 23, Switzerland.

I. INTRODUCTION

We have searched e^+e^- annihilation data at $\sqrt{s} = 29$ GeV from the MARK II detector^[1] at the PEP storage ring for events which may signify the existence of a new lepton doublet (L^-, L^0). We consider the case where the L^0 may be massive but does not exceed the L^- mass m_- . No evidence for a new lepton doublet was found.

Our analysis was motivated by the realization^{[2] [3]} that in searches for new sequential lepton pairs it had become conventional to set the L^0 mass m_0 to zero while considering ever more massive charged leptons. There is no real justification for this restriction and one should instead allow both m_- and m_0 to vary with the mass difference

$$\delta = m_- - m_0 \tag{1}$$

arbitrary. The present work is limited to

$$m_- > m_0 \tag{2}$$

and assumes that the (L^-, L^0) pair is subject to conventional weak interactions and that the L^0 is 'stable' in the sense that it is unlikely to decay within the MARK II detector, i.e. $\tau(L^0) \gtrsim 100$ ns. Neutrinos with masses between about $100 \text{ eV}/c^2$ and a few GeV/c^2 must be unstable in order to prevent the universe from having too large an energy density. However, our assumption that $\tau(L^0) \gtrsim 100$ ns does not conflict with the cosmological lifetime constraints.^[4] Recently Raby and West^[5] proposed a simple model with a stable Dirac L^0 of mass $m_0 \simeq 4 - 10 \text{ GeV}/c^2$ which, as well as solving the dark matter problem, also solves the solar neutrino problem if the standard neutral Higgs has a mass between 700 and 1000 MeV/c^2 .

The extent to which previous searches of e^+e^- data for new sequential leptons exclude lepton pairs with massive neutrinos has not been addressed quantitatively. If δ is small, a few GeV/c^2 or less for large m_- , the small visible energy in the signature events could cause them to be ignored in total cross-section measurements. When $\delta \lesssim m(\pi^-)$ the L^- has a long lifetime and would appear as a massive stable lepton in particle searches at PETRA. The absence of such leptons qualitatively excludes^[2] the $\delta \lesssim m(\pi^-)$ region for $m_- \lesssim 20 \text{ GeV}/c^2$ but no quantitative study has been made.

The largest existing lower limit on the mass of a new charged sequential lepton is $41 \text{ GeV}/c^2$, obtained by UA1^[6] from a study of W^\pm decays in $p\bar{p}$ annihilation.

This limit assumes that m_0 is near zero. Barnett and Haber^[7] re-examined this result and showed that smaller m_- mass ranges can be excluded for massive L^0 with $m_0 \lesssim 8 \text{ GeV}/c^2$. However, most of the (m_-, δ) plane cannot be excluded because large values of δ are needed to provide the visible L^- decay products with sufficient energy to separate them from the hadronic background.

The present search seeks to explore as much as possible of the (m_-, δ) plane and the small δ region in particular. The minimum accessible δ is limited by the increasing L^- lifetime and the decreasing momenta of the L^- decay products which eventually prevents the particle identification required for the signature events. The maximum accessible m_- is limited by the decreasing number of L^+L^- pairs which would be produced as m_- approaches E_{beam}/c^2 .

The decay modes which provide the best sensitivity at various δ values are discussed in Sec. II.C. The analysis method and data are described in Sec. III, and the resulting limits on the existence of new lepton pairs are given in Sec. IV.B.

II. PHYSICS OF NEW LEPTON PAIRS

A. Pair production

We assume that the L^- is a point particle obeying the Dirac equation. The production cross-section including radiative corrections at $\sqrt{s} = 29$ GeV is

$$\sigma(e^+e^- \rightarrow L^+L^-) = 68\beta(3 - \beta^2) \text{ pb} \quad (3)$$

where $\beta = \sqrt{1 - 4m_-^2/s}$.

B. Decay rates

We assume that the decays proceed through the conventional charged current weak interaction

$$\begin{aligned} L^- &\rightarrow L^0 + W^- \\ W^- &\rightarrow \text{other particles} \end{aligned} \quad (4)$$

with $(V - A)$ coupling at each W^- vertex. The occurrence of a particular decay mode requires the mass difference $\delta = m_- - m_0$ to be larger than the sum of the masses of the ‘other particles’ in Eq. (4). The branching fractions and decay kinematics for the allowed modes are controlled by δ and m_- , with δ having the major influence.

In the standard electroweak model, neglecting radiative corrections, the $(V - A)$ differential decay rate of L^- to L^0 and a fermion–anti-fermion pair is^[8]

$$\frac{d^4\Gamma(L^- \rightarrow L^0 \bar{f}_1 f_2)}{d\Omega_{f_2} d\phi_{\bar{f}_1 f_2} dx_{f_2} dx_{\bar{f}_1}} = \frac{G^2 m_-^5}{128\pi^5} \frac{\left[1 - x_{\bar{f}_1} + \frac{(m_{f_1}^2 - m_{f_2}^2 - m_0^2)}{m_-^2}\right] \left(x_{\bar{f}_1} - \frac{2s_L \cdot p_{\bar{f}_1}}{m_-}\right)}{\left\{ \left[1 + \frac{m_-^2(1 - x_{\bar{f}_1} - x_{f_2}) - m_0^2}{m_W^2}\right]^2 + \frac{\Gamma_W^2}{m_W^2} \right\}} \quad (5)$$

where G is the Fermi coupling constant, $x = 2E/m_-$ is the reduced energy variable, s_L is the 4-spin of L^- , $p_{\bar{f}_1}$ is the 4-momentum of \bar{f}_1 , and m_W and Γ_W are the mass and width of the W^- .

The physics of purely leptonic decays

$$L^- \rightarrow L^0 + \ell^- + \bar{\nu}_\ell \quad (6)$$

where $\ell = e, \mu, \tau$, follows directly from weak interaction theory and is described by Eq. (5), which was used in our Monte Carlo simulations.

The physics of single hadron decays

$$L^- \rightarrow L^0 + h^- \quad (7)$$

where $h = \pi, \rho, K, K^*, a_1$, follows from weak interaction theory and experimentally determined parameters such as the π^\pm lifetime and $\sigma(e^+e^- \rightarrow \rho^0)$. The $(V - A)$ differential decay rate for $L^- \rightarrow L^0\pi^-$ is^[9]

$$\frac{\Gamma(L^- \rightarrow L^0\pi^-)}{d\Omega_\pi} = \frac{G^2 f_\pi^2 \cos^2 \theta_c m_-^3}{64\pi^2} \{A(m_-, m_0, m_\pi) - s_L \cdot p_\pi B(m_-, m_0, m_\pi)\} \quad (8)$$

where p_π is the π^- 4-momentum, f_π is obtained from the $\pi^- \rightarrow \mu^- \bar{\nu}_\mu$ decay rate,^[10] θ_c is the Cabibbo angle, and

$$\begin{aligned} A(m_-, m_0, m_\pi) &= \frac{\sqrt{\Delta(m_-^2, m_0^2, m_\pi^2)} \{ (m_-^2 - m_0^2)^2 - m_\pi^2 (m_-^2 + m_0^2) \}}{m_-^6} \\ B(m_-, m_0, m_\pi) &= \frac{(m_-^2 - m_0^2) \Delta(m_-^2, m_0^2, m_\pi^2)}{m_-^6} \\ \Delta(x, y, z) &= x^2 + y^2 + z^2 - 2(xy + xz + yz) \end{aligned} \quad (8a)$$

Similarly, the $(V - A)$ decay rate for $L^- \rightarrow L^0\rho^-$ is

$$\frac{\Gamma(L^- \rightarrow L^0\rho^-)}{d\Omega_\rho} = \frac{G^2 f_\rho^2 \cos^2 \theta_c m_-^3}{64\pi^2} \{C(m_-, m_0, m_\rho) - s_L \cdot p_\rho D(m_-, m_0, m_\rho)\} \quad (9)$$

where p_ρ is the ρ^- 4-momentum and

$$\begin{aligned} C(m_-, m_0, m_\rho) &= \frac{\sqrt{\Delta(m_-^2, m_0^2, m_\rho^2)} \{ (m_-^2 - m_0^2)^2 + m_\rho^2 (m_-^2 + m_0^2) - 2m_\rho^4 \}}{m_-^6} \\ D(m_-, m_0, m_\rho) &= \frac{(m_-^2 - m_0^2 - 2m_\rho^2) \Delta(m_-^2, m_0^2, m_\rho^2)}{m_-^6} \end{aligned} \quad (9a)$$

There is no fundamental, general, and calculable method for describing the physics of decays with multiple hadrons such as $L^- \rightarrow L^0 + (n\pi)^-$ where $n > 2$ and $\pi = \pi^\pm, \pi^0$. When $\delta \gtrsim 4 \text{ GeV}/c^2$ it is conventional to treat these multi-hadron decays by assuming they occur through the subprocesses

$$\begin{aligned} L^- &\rightarrow L^0 + \bar{u} + d \\ L^- &\rightarrow L^0 + \bar{c} + s. \end{aligned} \quad (10)$$

Our Monte Carlo studies of the decays in Eq. (10) were simulated using Eq. (5) with constituent quark masses. The LUND fragmentation model^[11] was used to produce

the multi-hadron final states. This method was adopted for values of δ as small as m_τ . The single hadron decay modes of Eq. (7) were treated separately using Eqs. (8), (9), and (A3-7) of the Appendix, with non-zero resonance width effects included for the ρ^- , K^{*-} , and a_1^- . The decay modes and their partial widths are discussed in detail in the Appendix.

We now use the decay modes $L^- \rightarrow L^0 e^- \bar{\nu}_e$ and $L^- \rightarrow L^0 \pi^-$ to illustrate the dependence of the branching fractions and decay kinematics on m_- , m_0 , and $\delta = m_- - m_0$.

The decay width for $L^- \rightarrow L^0 e^- \bar{\nu}_e$ is

$$\Gamma(L^- \rightarrow L^0 e^- \bar{\nu}_e) = \frac{G^2 m_-^5}{192\pi^3} (1 - 8r + 8r^3 - r^4 - 12r^2 \ln r) \quad (11)$$

where $r \equiv (m_0/m_-)^2$, and the e and ν_e masses are taken to be zero.

The decay width for $L^- \rightarrow L^0 \pi^-$ is

$$\Gamma(L^- \rightarrow L^0 \pi^-) = \frac{G^2 f_\pi^2 \cos^2 \theta_c m_-^3}{16\pi} A(m_-, m_0, m_\pi) \quad (12)$$

When $m_0 = 0$ we obtain the usual threshold term $A = (1 - m_\pi^2/m_-^2)^2$ from Eq. (8a).

As m_- increases with δ held constant the decay widths are dominated by δ . In the limit $m_- \rightarrow \infty$, and $\delta \ll m_-$, the decay widths become

$$\Gamma(L^- \rightarrow L^0 e^- \bar{\nu}_e) = \frac{G^2 \delta^5}{15\pi^3} \quad (13)$$

$$\Gamma(L^- \rightarrow L^0 \pi^-) = \frac{G^2 f_\pi^2 \cos^2 \theta_c \delta^3}{4\pi} (1 - m_\pi^2/\delta^2)^{1/2} (1 - m_\pi^2/2\delta^2). \quad (14)$$

Figure 1 shows the dependence of the branching fractions on δ for $m_- = 2 \text{ GeV}/c^2$ and $10 \text{ GeV}/c^2$.

C. Event signatures

The event signatures were chosen to provide sensitivity over as much of the (m_-, δ) plane as possible and to reject the large numbers of Bhabha events ($e^+e^- \rightarrow e^+e^-$), μ -pair events ($e^+e^- \rightarrow \mu^+\mu^-$), and hadronic events ($e^+e^- \rightarrow \text{hadrons}$). Suitable signatures consist of L^+L^- decays to $e^\pm\mu^\mp$, as in the discovery of the τ lepton,^[12]

or L^\pm decay to e^\pm or μ^\pm and L^\mp decay to hadrons. The main backgrounds to any new-lepton-pair events are then from τ -pair production ($e^+e^- \rightarrow \tau^+\tau^-$), and two-virtual-photon reactions. We use the following decay modes:

$$\begin{aligned}
L^- &\rightarrow L^0 + e^- + \bar{\nu}_e \\
L^- &\rightarrow L^0 + \mu^- + \bar{\nu}_\mu \\
L^- &\rightarrow L^0 + \pi^- \\
L^- &\rightarrow L^0 + \rho^- \\
L^- &\rightarrow L^0 + a_1^- \\
L^- &\rightarrow L^0 + (\geq 3 h^\pm)^- + \geq 0 \gamma
\end{aligned} \tag{15}$$

where $h = \pi$ or K to form the event signatures:

$$e^+ + e^- \rightarrow e^\pm + \mu^\mp + E_{miss} \tag{16a}$$

$$e^+ + e^- \rightarrow e^\pm + \pi^\mp + \leq 4 \gamma + E_{miss} \tag{16b}$$

$$e^+ + e^- \rightarrow \mu^\pm + \pi^\mp + \leq 4 \gamma + E_{miss} \tag{16c}$$

$$e^+ + e^- \rightarrow e^\pm + (\geq 3 h^\pm)^\mp + \geq 0 \gamma + E_{miss} \tag{16d}$$

$$e^+ + e^- \rightarrow \mu^\pm + (\geq 3 h^\pm)^\mp + \geq 0 \gamma + E_{miss} \tag{16e}$$

where E_{miss} is the missing energy carried away by unobserved particles.

The ranges of δ for which large numbers of signature events are expected can be inferred from Fig. 1. For example, the branching fractions to e and μ both exceed 10% if $\delta \gtrsim 0.5 \text{ GeV}/c^2$ so at least 2% of these L^+L^- pairs would decay to the $e^\pm\mu^\mp$ signature of Eq. (16a). Similarly, the event signatures of Eq. (16b, c) and Eq. (16d, e) are significant for $0.2 \lesssim \delta \lesssim 3 \text{ GeV}/c^2$ and $\delta \gtrsim 1.5 \text{ GeV}/c^2$ respectively. However if δ is small, and especially if also m_- is large, the decay products may not have sufficient momentum to allow the particle identification required for these signatures.

III. ANALYSIS METHOD AND DATA

A. The visible energy problem

In general purpose magnetic detectors used at e^+e^- colliders the visible energy E_{vis} measured in an event is the sum of up to three components: the total energy of the charged particles with measured momentum; the total energy of photons detected in electromagnetic energy calorimeters; and, if hadronic energy calorimeters are present, the additional energy of detected neutrons and K^0 's. The energy carried by neutrinos and other undetected particles is, of course, absent from E_{vis} . With the assumption of a stable L^0 the sum of the visible energies from each decaying L^\pm pair is

$$\begin{aligned} E_{vis} &= E_{vis,1} + E_{vis,2} \\ E_{vis,i} &\leq E_{beam} - E_{0,i} \quad i = 1, 2 \end{aligned} \tag{17}$$

where the E_0 's are the energies carried off by the L^0 's. Figure 2 illustrates the visible energy spectrum, without detector acceptance effects, from $L^- \rightarrow L^0 + \text{multi-hadrons}$ for various δ values when $E_{beam} = 14.5$ GeV and $m_- = 10$ GeV/ c^2 .

Previous searches for new charged leptons in e^+e^- annihilation always required that E_{vis} be greater than several or many GeV. This requirement eliminates most events from the two-virtual-photon reactions

$$e^+e^- \rightarrow e^+e^-x^+x^- \tag{18}$$

where $x = e, \mu, \pi, K$. Indeed a minimum E_{vis} cut is used in most studies of e^+e^- annihilation physics for the same reason. The effect of the minimum E_{vis} cut in previous analyses was to exclude searches for lepton pairs with $\delta \lesssim 4$ GeV/ c^2 when m_- is large. Our analysis method allows us to search for lepton pairs with δ as small as 1 GeV/ c^2 or less.

B. Data

We use $\sqrt{s} = 29$ GeV e^+e^- annihilation data obtained at PEP with the MARK II detector in its 'pre-upgrade' configuration^[1] during 1981-1984. The data analysed for each event signature was (205.1 ± 3.0) pb $^{-1}$ for Eq. (16a), (104.0 ± 1.6) pb $^{-1}$ for Eqs. (16b, c), and (123.8 ± 1.8) pb $^{-1}$ for Eqs. (16d, e).

C. Backgrounds from known processes

Backgrounds from known processes which contribute to the event signatures of Eqs. (16a-e) were calculated from Monte Carlo simulations which included the acceptances and efficiencies of the MARK II detector. The background sources discussed in the rest of this section were considered.

1. $e^+e^- \rightarrow \tau^+\tau^-$

The process $e^+e^- \rightarrow \tau^+\tau^-$ is the dominant source of background to the event signatures in Eqs. (16a-e). The backgrounds were determined from simulated events corresponding to an integrated luminosity of 817 pb^{-1} . The τ -pair background estimates assumed the branching fractions and normal errors shown in Table I.

2. $e^+e^- \rightarrow \text{hadrons}$

The reaction $e^+e^- \rightarrow q\bar{q} \rightarrow \text{hadrons}$ can produce signature events through the decay of a hadron to an e or μ , or through the misidentification of a hadron as an e or μ . The simulated events corresponded to an integrated luminosity of 192 pb^{-1} . The extent to which the LUND fragmentation model used for the intermediate stages of the reaction, where many quarks and gluons are produced and hadronized, correctly simulates small multiplicity events is of some concern. However the predicted hadronic backgrounds are very small or zero, as shown in Tables II through VI, and no estimate of model-dependent uncertainties are made.

3. $e^+e^- \rightarrow e^+e^-\mu^+\mu^-$

Events from the two-virtual-photon reaction $e^+e^- \rightarrow e^+e^-\mu^+\mu^-$ were simulated using the Monte Carlo programs of Berends *et al.*^[18] The generated events corresponded to an integrated luminosity of 410 pb^{-1} .

4. $e^+e^- \rightarrow e^+e^-\tau^+\tau^-$

The two-virtual-photon production of τ pairs can contribute to the signature events in two ways. Using (ℓ) to denote a lepton which is not observed in the central region of the detector, usually because the angle between its path and the beamline is too small, the two possibilities are

$$e^+e^- \rightarrow (e^+)(e^-\ell^+\ell^-) \quad (19a)$$

$$e^+e^- \rightarrow (e^\pm)e^\mp\tau^\pm(\tau^\mp) \quad (19b)$$

where the former is the more likely. Again, the events were simulated using the programs of Berends *et al.*^[18]

$$5. e^+e^- \rightarrow e^+e^- + \text{hadrons}$$

The most uncertain calculation of the background from a known process concerns the set of two-virtual-photon reactions

$$e^+e^- \rightarrow e^+e^- + \text{hadrons}. \quad (20)$$

The methods of Ref. 13 were applied to

$$\begin{aligned} e^+e^- &\rightarrow e^+e^-q\bar{q} \\ q + \bar{q} &\rightarrow \text{hadrons} \end{aligned} \quad (21)$$

where q is a $u, d, s, c,$ or b quark. However, this is not a good model when the invariant mass of the hadrons is about $1 \text{ GeV}/c^2$ or less. A better model for that region would be

$$\begin{aligned} e^+e^- &\rightarrow e^+e^-\gamma_v\gamma_v \\ \gamma_v + \gamma_v &\rightarrow \text{hadrons} \end{aligned} \quad (22)$$

where γ_v is a virtual photon, but we do not have a Monte Carlo program for this model.

The two-virtual-photon processes may be studied experimentally with the MARK II's small angle tagging (SAT) system. One can select SAT-tagged two-virtual-photon events of the form

$$e^+e^- \rightarrow e_{SAT}^\pm + \text{signature particles} \quad (23)$$

where e_{SAT}^\pm denotes an electron detected by the SAT.

Two-virtual-photon backgrounds may also be studied by selecting signature events in which the lepton charge is the same as, instead of opposite to, the charge of the other particles. The 'same-charge' and 'opposite-charge' backgrounds should be the same for $e^+e^- \rightarrow e^+e^-\mu^+\mu^-$, and similar for $e^+e^- \rightarrow e^+e^-q\bar{q}$ if one of the electrons is usually the observed lepton. The 'same-charge' analog of Eq. (19b), i.e. $e^+e^- \rightarrow (e^\pm)e^\mp(\tau^\pm)\tau^\mp$, also contributes to the 'same-charge' background. Hadronic and τ -pair events may

contribute if some charged particles are unobserved or if the charge of one particle is measured incorrectly.

Both methods were used to check the Monte Carlo predictions of the two-virtual-photon backgrounds. The results are given in Sec. IV.A.

6. $e^+e^- \rightarrow \mu^+\mu^- + \text{hadrons}$

The backgrounds from the two-virtual-photon reaction $e^+e^- \rightarrow \mu^+\mu^- + \text{hadrons}$ were determined from Monte Carlo simulations based on Ref. 13.

7. $e^+e^- \rightarrow e^+e^-(\gamma)$

The backgrounds from Bhabha and radiative Bhabha scattering $e^+e^- \rightarrow e^+e^-(\gamma)$ were determined from a Monte Carlo simulation, corresponding to an integrated luminosity of 90 pb^{-1} , based on the work of Berends and Kleiss.^[14]

8. $e^+e^- \rightarrow \mu^+\mu^-(\gamma)$

The backgrounds from single photon production of muon pairs $e^+e^- \rightarrow \mu^+\mu^-(\gamma)$ were determined from a Monte Carlo simulation, based on the work of Berends and Kleiss^[15] corresponding to an integrated luminosity of 317 pb^{-1} .

D. Selection of signature events

The criteria for the signature events use accepted charged particles and photons defined as follows. An accepted charged track must be measured in the main drift chamber, satisfy track quality and vertex criteria, and have a measured momentum $p > 0.1 \text{ GeV}/c$. An accepted photon must satisfy measurement quality criteria in the LA calorimeter, have a measured energy $E > 0.2 \text{ GeV}$, and be separated from all charged particle tracks at the inner face of the calorimeter by at least 0.2 m unless the photon energy exceeds the charged track energy.

Lepton identification was attempted for charged tracks with $p > 0.5 \text{ GeV}/c$. Identified electrons satisfied shower development criteria within the fiducial volume of the LA calorimeter. Identified muons penetrated at least two of the four layers of the muon identification system and satisfied hit pattern criteria. Muon identification was possible for tracks with $p > 1 \text{ GeV}/c$. Lepton identification efficiency corrections of 0.96 ± 0.01 for electrons and 0.97 ± 0.01 for muons were applied to the Monte Carlo simulations.

We denote the number of accepted charged particles by n_c , the number of identified leptons (e or μ) by n_l , the number of accepted photons by n_γ , and the total charge in an event by Q . Accepted events had at least two charged tracks with $\cos\theta < 0.65$ with respect to the beam direction.

Three types of event signatures were used: $e\mu$ pairs, $\ell\pi$ pairs ($\ell = e, \mu$) with ≤ 4 photons associated with the π^\pm , and isolated lepton versus multihadron events, corresponding to Eqs. (16a), (16b, c), and (16d, e), respectively. These event types were divided into a total of 18 subtypes, which are defined and whose purpose is explained in the remainder of this section.

1. $e\mu$ events

As in the discovery of the τ lepton, $e^\pm\mu^\mp$ pairs are a good signature for new lepton pairs. We require $n_c = 2$ with one identified e and one identified μ , $n_\gamma = 0$, and $Q = 0$. Events in which the e has $p < 1.25$ GeV/c and the μ penetrates less than three layers of the muon system were not accepted. The $e\mu$ events are divided into two subtypes, one with acollinearity angle $\theta_{acol} < 25^\circ$ and the other with $\theta_{acol} > 25^\circ$. Most $e\mu$ events from $e^+e^- \rightarrow \tau^+\tau^-$ are in the $\theta_{acol} < 25^\circ$ subtype. The $\theta_{acol} < 25^\circ$ subtype is more important for small δ and small m_- while the $\theta_{acol} > 25^\circ$ subtype is more important when δ is large and m_- is close to E_{beam}/c^2 .

2. $\ell\pi$ Events

The accepted $\ell\pi$ events had $n_c = 2$ with only one identified e or μ , $n_\gamma \leq 4$, and $Q = 0$. Accepted events had $p_e > 0.5$ GeV/c or $p_\mu > 1$ GeV/c, and $p_\pi > 1$ GeV/c. Additional sets of criteria had to be satisfied depending on whether $n_\gamma = 0$ or $n_\gamma > 0$.

In the $n_\gamma = 0$ case, special care was taken to reject backgrounds from Bhabha or muon pair events where one of the leptons is misidentified as a pion. Accepted π^\pm passed strict lepton rejection cuts in both the LA calorimeter and the muon system. Both charged tracks were required to have $p < 13.0$ GeV/c. A pion identification efficiency correction of 0.87 ± 0.03 , based on studies of 3-prong τ decays, was applied to the Monte Carlo simulations. Events in which the acoplanarity angle between the planes defined by each of the charged tracks and the beam direction was less than 2° were rejected.

In the $n_\gamma > 0$ case, the candidate π^\pm were charged tracks not identified as leptons. In accepted events the π^\pm formed a reconstructed ρ^\pm with the photons, the total energy

of the π^\pm and photons was less than 14.5 GeV, and the photons were isolated from the lepton by $\cos \theta_{\ell\gamma} < 0.85$. For $n_\gamma = 1$, we required $E_\gamma > 2.0$ GeV; $p_e < 11.0$ GeV/c in $e\pi(1\gamma)$ events to reject Bhabha events in which the other electron radiates the observed photon and is misidentified as a pion; and a reconstructed ρ^\pm from the π^\pm and γ when the γ is 'replaced' by a π^0 of the same momentum. For $n_\gamma = 2$ or 3 accepted events contained a reconstructed π^0 from two photons, and a reconstructed ρ^\pm from the π^\pm and the two photons. For $n_\gamma = 4$ accepted events contained two reconstructed π^0 's from the four photons; a reconstructed ρ^\pm from the π^\pm and the photons of one of the reconstructed π^0 's; and a reconstructed a_1^\pm from the π^\pm and the four photons. The acceptable masses of reconstructed π^0 , ρ^\pm , and a_1^\pm were $0.04 < m(\pi^0) < 0.24$ GeV/c², $0.4 < m(\rho^\pm) < 1.1$ GeV/c², and $0.75 < m(a_1^\pm) < 1.8$ GeV/c².

The $\ell\pi$ events are divided into the types $e\pi$ and $\mu\pi$ for $n_\gamma = 0$, and $e\pi(n_\gamma)$ and $\mu\pi(n_\gamma)$ for $n_\gamma > 0$. These event types are further divided into $\theta_{acol} < 25^\circ$ and $\theta_{acol} > 25^\circ$ subtypes, where θ_{acol} is the acolinearity angle of the e^\pm and π^\mp for $n_\gamma = 0$, the e^\pm and reconstructed ρ^\mp for $n_\gamma = 1, 2, 3$, and the e^\pm and a_1^\mp for $n_\gamma = 4$. Most $\ell\pi$ events from $e^+e^- \rightarrow \tau^+\tau^-$ are in the $\theta_{acol} < 25^\circ$ subtypes.

3. Isolated lepton events

The isolated lepton event signature has the following properties:

- (a) $n_\ell = 1$, $\ell = e$ or μ with $1.25 < p < 14.0$ GeV/c,
- (b) the angle between the lepton and each other accepted charged track or photon is $> 90^\circ$; hence the term isolated lepton,
- (c) the total energy of all accepted charged particles and photons in the hemisphere opposite to the isolated lepton is < 14.0 GeV,
- (d) $n'_c \geq 3$, where n'_c is the number of charged particles, excluding the isolated lepton and particles having the kinematic properties of an e^+e^- pair from photon conversion,
- (e) all the n'_c tracks which enter the end-cap calorimeter deposit too little energy to be identified as electrons,
- (f) $Q = 0$ if $n'_c = 3$.

The invariant mass m_{inv} of the charged particles and photons in the hemisphere opposite the isolated lepton is used, together with n'_c , to divide the events into four subtypes. The isolated electron events are divided into the types $e3$ for $n'_c = 3$ and $e > 3$ for $n'_c > 3$. These event types are further divided into $m_{inv} < 2.5$ GeV/c² and $m_{inv} > 2.5$ GeV/c² subtypes. The analogous isolated muon event types are denoted by $\mu3$ and

$\mu > 3$. The partition of the invariant mass m_{inv} at $2.5 \text{ GeV}/c^2$ puts most $e^+e^- \rightarrow \tau^+\tau^-$ isolated lepton events into the $e3$ and $\mu3$ subtypes with $m_{inv} < 2.5 \text{ GeV}/c^2$. The partition point is greater than m_τ to allow for measurement errors.

IV. RESULTS AND CONCLUSIONS

A. Numerical results

The numbers of events found in the data for the signature subtypes described in Sec. III.D are shown in the first rows of Tables II through VI. The expected numbers of background events from the known sources discussed in Sec. III.C are also shown. Background sources for which the Monte Carlo simulations predict zero events are omitted from the Tables. The normal errors shown for the expected backgrounds are the statistical errors added in quadrature with estimates of systematic uncertainties in the integrated luminosities of the data sets (Sec. III.B), the relative particle identification efficiencies in the data and the Monte Carlo simulations (Sec. III.D), and the uncertainties in the τ branching fractions (Table I) where relevant. The statistical error in the number of background events is

$$\sigma = \sqrt{N}(1 + \mathcal{L}_D/\mathcal{L}_{MC})^{1/2} \quad (24)$$

where N is the number of events predicted in a data set with integrated luminosity \mathcal{L}_D by a Monte Carlo simulation with integrated luminosity \mathcal{L}_{MC} .

The Monte Carlo predictions of two-virtual-photon backgrounds may be checked using ‘SAT-tagged’ events and ‘same-charge’ events, as discussed in Sec. III.C.5. Table VII shows the numbers of these events found in the data and the Monte Carlo simulations for each event subtype. The two-virtual-photon Monte Carlo simulations predict 16.6 ± 6.2 SAT-tagged events compared to 32 events observed in the data. The ‘same-charge’ method was applied to all event subtypes except the $e > 3$ and $\mu > 3$ subtypes where the number of charged tracks n_c could be odd and the total charge was not restricted (Sec. III.D.3). The Monte Carlo simulations predict 4.8 ± 2.3 ‘same-charge’ events from $e^+e^- \rightarrow \tau^+\tau^-$, 0.5 ± 0.9 from $e^+e^- \rightarrow \text{hadrons}$, 4.2 ± 3.1 from $e^+e^- \rightarrow e^+e^-\tau^+\tau^-$, 13.0 ± 4.4 from $e^+e^- \rightarrow e^+e^-\mu^+\mu^-$, 4.8 ± 2.3 from $e^+e^- \rightarrow e^+e^-q\bar{q}$, and 1.0 ± 1.4 from $e^+e^- \rightarrow \mu^+\mu^-q\bar{q}$ giving a predicted total of 28.3 ± 6.5 ‘same-charge’ events compared to 34 events observed in the data. The ‘same-charge’ method therefore finds the predicted two-virtual-photon background to be in fairly good agreement with the data, whereas the ‘SAT-tagged’ method suggests that it may be underestimated. It should be noted that underestimated backgrounds give weaker limits for excluding new lepton pairs.

The number of ‘excess events’ shown in the bottom row of each of Tables II through VI is the difference between the number of data events and the sum of the expected backgrounds. The total number of data events is 1277 while the total expected background is 1234.4 ± 46.8 where the errors have been added in quadrature. The individual numbers of ‘excess events’ are generally consistent with zero, except for the two $e > 3$ event subtypes which contribute 11.9 to the total $\chi^2 = 26.8$ for 18 degrees of freedom. We do not know if the significant numbers of ‘excess events’ in the $e > 3$ subtypes are statistical fluctuations or are due to deficiencies in the analysis method or to physics we do not understand.

B. Limits on new lepton pairs

Having found no significant evidence for new lepton pairs, we next determine the (m_-, δ) region excluded by the results in Tables II through VI. Monte Carlo simulations of (L^-, L^0) production and decay were made at 33 points in the (m_-, δ) plane. The simulations included the physics discussed in Sec. II and the Appendix. The Monte Carlo events were analyzed for each of the signature event subtypes described in Sec. III.D.

For each event subtype and at each (m_-, δ) Monte Carlo simulation point a probability ratio method is used to compare the likelihoods for the following two hypotheses: (i) the data is consistent with the expected background alone, and (ii) the data is consistent with the expected background plus the predicted number of new-lepton-pair events. Gaussian probability distributions

$$G(x; \mu, \sigma) = (2\pi\sigma^2)^{-1/2} \exp[-(x - \mu)^2/2\sigma^2] \quad (25)$$

are used for simplicity. The unphysical $x < 0$ regions are excluded and remaining $x \geq 0$ regions normalized to unit area by multiplying the probability distribution by

$$C = \left[\int_0^{\infty} G(x; \mu, \sigma) dx \right]^{-1}. \quad (26)$$

Denoting the number of data events in the i 'th subtype by N_i , the expected background by $\mu_B \pm \sigma_B$, and the expected background plus the predicted number of new-lepton-pair

events at (m_-, δ) by $\mu_L \pm \sigma_L$, the desired probability ratio is

$$R_i = \frac{C_B G(N; \mu_B, \sigma_B)}{C_L G(N; \mu_L, \sigma_L)}. \quad (27)$$

If $R_i > 1$, the ‘background alone’ hypothesis is favored. Figures 3, 4, and 5 show $R_i = 9$ contours obtained by interpolating between, or extrapolating from, the R_i values at the (m_-, δ) simulation points. The hatched regions show the parts of the (m_-, δ) plane in which new lepton pairs are excluded with $R_i > 9$.

The most restrictive limits are from the $e\mu$ event type, and at small δ from the $e\pi$ event type. The $\mu\pi$ subtypes exclude smaller regions than the $e\pi$ subtypes primarily because electron identification was possible for smaller momenta than for muon identification (see Sec. III.D). No part of the (m_-, δ) plane was excluded with $R_i > 9$ by the $\mu\pi(n\gamma)$ subtype with $\theta_{acol} > 25^\circ$. The bulges toward large δ at large m_- in the $e\pi$ and $\mu\pi$ subtypes with $\theta_{acol} > 25^\circ$ appear to be due to L^\pm decay to several pions where only one π^\pm is at a large enough angle from the beamline to be detected. In the isolated lepton events the more restrictive limits at small δ are from the low multiplicity $e3$ and $\mu3$ subtypes with $m_{inv} < 2.5 \text{ GeV}/c^2$.

The product of the individual probability ratios R_i for the 18 event subtypes gives the combined probability ratio

$$R = \prod_{i=1}^{18} R_i \quad (28)$$

shown in Table VIII for each of the 33 (m_-, δ) Monte Carlo simulation points. The ‘background alone’ hypothesis was favored at all (m_-, δ) simulation points except $(0.3, 0.3) \text{ GeV}/c^2$, for which $R = 0.92$, and $(13, 0.7) \text{ GeV}/c^2$, for which $R = 1.0$. Figure 6 shows the $R = 9$ contour and hatched region corresponding to $R > 9$ on both linear and logarithmic δ scales. The $R = 99$ contour is also shown on the logarithmic δ scale.

C. Tau branching fractions

— If new lepton pairs with $m_- < 14.5 \text{ GeV}/c^2$ are assumed not to exist the results in Tables II through VI may be used to obtain values for the τ branching fractions. The isolated lepton event subtypes (Sec. III.D.3) other than $e3$ and $\mu3$ with $m_{inv} < 2.5 \text{ GeV}/c^2$ are not used since the numbers of τ -pair decays in those subtypes are negligible.

The best estimate of the true number of τ -pair events N_τ in each of the remaining 12 event subtypes is given by the observed number of events minus the sum of the expected backgrounds other than $e^+e^- \rightarrow \tau^+\tau^-$. The expected $e^+e^- \rightarrow \tau^+\tau^-$ backgrounds in the second row of Tables II through VI assumed the branching fractions shown in Table I. The branching fractions giving τ -pair backgrounds agreeing most closely with the N_τ events were found by performing a global χ^2 fit over the 12 event subtypes using the MINUIT^[16] minimization program. The best fit τ branching fractions, for which $\chi^2 = 5.4$ for 7 degrees of freedom, are shown in Table IX. The normal errors include the statistical errors and the estimated uncertainties in the integrated luminosity and particle identification efficiencies but do not include any other systematic uncertainties in the predicted number of background events. The last decay mode shown in Table IX combines the last two decay modes shown in Table I because the $e\pi(n\gamma)$ and $\mu\pi(n\gamma)$ subtypes (Sec. III.D.2) sum over events with from 1 to 4 observed photons. The τ branching fractions obtained from the present analysis are in good agreement with currently accepted branching fractions. A detailed statistical study of τ decay data has recently been performed by Hayes and Perl.^[17]

D. Conclusions

In conclusion, we have found no evidence for new lepton pairs (L^-, L^0) in our 29 GeV e^+e^- annihilation data and have excluded their existence over most of the accessible (m_-, δ) plane. The data, with the possible exception of the $e > 3$ event subtypes, appear to be consistent with known processes and with the currently accepted τ branching fractions.

APPENDIX: L^- BRANCHING FRACTIONS

Decay width formulae for heavy charged leptons were calculated by Tsai^[10] assuming massless neutrinos. This section gives the generalized formulae for the case where the L^0 is massive but does not exceed the L^- mass. The W^\pm propagator effects included in Eq. (5) are neglected here.

The decay width for $L^- \rightarrow L^0 e^- \bar{\nu}_e$ is

$$\Gamma(L^- \rightarrow L^0 e^- \bar{\nu}_e) = \frac{G^2 m_-^5}{192\pi^3} (1 - 8r + 8r^3 - r^4 - 12r^2 \ln r) \quad (\text{A1})$$

where G is the Fermi coupling constant, $r \equiv (m_0/m_-)^2$, and the e and ν_e masses are assumed to be negligible.

The decay width for $L^- \rightarrow L^0 \mu^- \bar{\nu}_\mu$, where only the ν_μ mass is assumed to be negligible, is^[10]

$$\begin{aligned} \Gamma(L^- \rightarrow L^0 \mu^- \bar{\nu}_\mu) = & \frac{G^2 m_-^5}{192\pi^3} \left\{ \frac{1}{2} [2 - 3s^3 - s^2 + (5D - 14)s - 13D] r \right. \\ & \left. - \frac{3}{2} [s^4 - 2(D + 2)s^2 + D^2 - 4D] L_1 + 12s\sqrt{D} L_2 \right\} \end{aligned} \quad (\text{A2})$$

where

$$\begin{aligned} s & \equiv \frac{m_\mu^2 + m_0^2}{m_-^2} \\ D & \equiv \frac{(m_\mu^2 - m_0^2)^2}{m_-^4} \\ r & \equiv \sqrt{1 - 2s + D} \\ L_1 & \equiv \ln \frac{(1 - s + r)m_-^2}{2m_\mu m_0} \\ L_2 & \equiv \ln \frac{(s - D - \sqrt{D}r)m_-^2}{2m_\mu m_0}. \end{aligned} \quad (\text{A2a})$$

The decay width for $L^- \rightarrow L^0 \tau^- \bar{\nu}_\tau$ is obtained by replacing m_μ by m_τ in Eqs. (A2) and (A2a).

The following decay width formulae for L^- decays to a single scalar or vector hadron are valid in the narrow resonance limit. For resonances of finite width the threshold terms should be averaged over q^2 , where q is the hadron 4-momentum. For the long-lived scalar hadrons π^\pm and K^\pm one need only substitute m^2 for q^2 . The

decay width for $L^- \rightarrow L^0 \pi^-$ is^[9]

$$\Gamma(L^- \rightarrow L^0 \pi^-) = \frac{G^2 f_\pi^2 m_-^3 \cos^2 \theta_c \sqrt{\Delta} \{ (m_-^2 - m_0^2)^2 - q_\pi^2 (m_-^2 + m_0^2) \}}{16\pi m_-^6} \quad (\text{A3})$$

where θ_c is the Cabibbo angle, q_π is the pion 4-momentum and

$$\begin{aligned} \Delta &= \Delta(m_-^2, m_0^2, q_\pi^2) \\ \Delta(x, y, z) &= x^2 + y^2 + z^2 - 2(xy + xz + yz) \end{aligned} \quad (\text{A3a})$$

The decay width for $L^- \rightarrow L^0 K^-$ is

$$\Gamma(L^- \rightarrow L^0 K^-) = \frac{G^2 f_K^2 m_-^3 \sin^2 \theta_c \sqrt{\Delta} \{ (m_-^2 - m_0^2)^2 - q_K^2 (m_-^2 + m_0^2) \}}{16\pi m_-^6} \quad (\text{A4})$$

The threshold factor for the decay to a single vector hadron differs from that for decay to a single scalar hadron. The decay width for $L^- \rightarrow L^0 \rho^-$ is^[19]

$$\Gamma(L^- \rightarrow L^0 \rho^-) = \frac{G^2 f_\rho^2 m_-^3 \cos^2 \theta_c \sqrt{\Delta} \{ (m_-^2 - m_0^2)^2 + q_\rho^2 (m_-^2 + m_0^2) - 2q_\rho^4 \}}{16\pi m_-^6} \quad (\text{A5})$$

where $m_\rho = 770 \text{ MeV}/c^2$ and $\Delta = \Delta(m_-^2, m_0^2, q_\rho^2)$.

The decay width for $L^- \rightarrow L^0 a_1^-$ is

$$\Gamma(L^- \rightarrow L^0 a_1^-) = \frac{G^2 f_{a_1}^2 m_-^3 \cos^2 \theta_c \sqrt{\Delta} \{ (m_-^2 - m_0^2)^2 + q_{a_1}^2 (m_-^2 + m_0^2) - 2q_{a_1}^4 \}}{16\pi m_-^6} \quad (\text{A6})$$

where $\Delta = \Delta(m_-^2, m_0^2, q_{a_1}^2)$ and the Weinberg sum rules^[20] give the relation $m_\rho f_\rho = m_{a_1} f_{a_1}$.

The decay width for $L^- \rightarrow L^0 K^{*-}$ is

$$\Gamma(L^- \rightarrow L^0 K^{*-}) = \frac{G^2 f_{K^*}^2 m_-^3 \sin^2 \theta_c \sqrt{\Delta} \{ (m_-^2 - m_0^2)^2 + q_{K^*}^2 (m_-^2 + m_0^2) - 2q_{K^*}^4 \}}{16\pi m_-^6} \quad (\text{A7})$$

where $\Delta = \Delta(m_-^2, m_0^2, q_{K^*}^2)$ and the DMO sum rules^[21] give the relation $f_\rho = f_{K^*}$.

The decay width for $L^- \rightarrow L^0 \bar{u}d \rightarrow \text{hadron continuum}$ is^[19]

$$\Gamma(L^- \rightarrow L^0 \bar{u}d) = \frac{3G^2 m_-^5}{192\pi^3} 8r \left\{ r \left(\frac{-2 \sin \theta_\Lambda}{\cos^4 \theta_\Lambda} - \frac{\sin \theta_\Lambda}{\cos^2 \theta_\Lambda} + 3 \ln |\sec \theta_\Lambda + \tan \theta_\Lambda| \right) + 2\sqrt{r}(1+r) \tan^3 \theta_\Lambda \right\} \quad (\text{A8})$$

where

$$\begin{aligned} r &\equiv (m_0/m_-)^2 \\ \sec \theta_\Lambda &\equiv \frac{1+r-x_\Lambda}{2\sqrt{r}} \\ x_\Lambda &= (\Lambda/m_-)^2 \\ 0 &\leq \theta_\Lambda \leq \pi/2 \end{aligned} \quad (\text{A8a})$$

and Λ is minimum invariant mass cut-off for the $\bar{u}d$ hadronic continuum. The decay width for $L^- \rightarrow L^0 \bar{c}s \rightarrow \text{hadron continuum}$ is also given by Eq. (A8), but with a larger Λ in Eq. (A8a). It should be noted that in the limit $x_\Lambda \rightarrow 0$ Eq. (A8) reduces to

$$\Gamma(L^- \rightarrow L^0 \bar{u}d) = 3\Gamma(L^- \rightarrow L^0 e^- \bar{\nu}_e) \quad (\text{A9})$$

where 3 is the color factor. Braaten^[22] has recently calculated perturbative QCD corrections to the color factor in heavy lepton decay, and found $\Gamma(\tau^- \rightarrow \nu_\tau + \text{hadrons})/\Gamma(\tau^- \rightarrow \nu_\tau e^- \bar{\nu}_e) = 3.29 \pm 0.04$ while a ratio^[23] of $3(1 + \alpha_s/\pi)$ is appropriate for very large m_- and δ . Our Monte Carlo simulations assumed the naive value of 3 for the color factor.

Equations (A1-8) give the dependence of the decay widths on m_- and m_0 . In calculating the branching fractions for L^- decay the normalizations in Eqs. (A3-7) were adjusted relative to Eq. (1) to give good agreement with the τ decay branching fractions for $m_- = 1.784 \text{ GeV}/c^2$ and $m_0 = 0$. The normalization of Eq. (A8) relative to Eq. (A1) was retained, so as to preserve Eq. (A9) in the small x_Λ limit. Good agreement with the τ decay branching fractions was obtained by setting the minimum invariant mass for the $\bar{u}d$ hadron continuum states to $\Lambda = 1.275 \text{ GeV}/c^2$. We set $\bar{\Lambda} = 2.0 \text{ GeV}/c^2$ for the $\bar{c}s$ hadron continuum states.

REFERENCES

1. R.H. Schindler *et al.*, *Phys. Rev. D* 24, 78, (1981).
2. M.L. Perl, Proc. XXIII Int. Conf. High Energy Physics (Berkeley, 1986), ed. S.C. Loken, p.596.
3. D.P. Stoker and M.L. Perl, Proc. Leptonic Session 22nd Rencontre de Moriond, 1987, Vol. 1., p.445.
4. D.A. Dicus, E.W. Kolb, and V.L. Teplitz, *Phys. Rev. Lett.* 39, 168 (1977).
5. S. Raby and G.B. West, *Phys. Lett.* B202, 47 (1988); for an earlier model see *Nucl. Phys.* B292, 793 (1987).
6. C. Aljabar *et al.*, *Phys. Lett.* B185, 241 (1987).
7. R.M. Barnett and H.E. Haber, *Phys. Rev. D* 36, 2042 (1987).
8. B.F.L. Ward, *Phys. Rev. D* 35, 2092, (1987) contains formulae, from which our Eq. (5) was derived, for the differential decay rates of gauge-Higgs fermions associated with the minimal supersymmetry extension of the standard model. The angular notation is illustrated in Fig. 8 of this reference.
9. J. Babson and E. Ma, *Phys. Rev. D* 26, 2497 (1982).
10. Y.S. Tsai, *Phys. Rev. D* 4, 2821 (1971).
11. T. Sjöstrand, *Comp. Phys. Comm.* 39, 347 (1986); T. Sjöstrand and M. Bengtsson, *ibid.* 43, 367 (1987).
12. M.L. Perl *et al.*, *Phys. Rev. Lett.* 35, 1489 (1975).
13. F.A. Berends, P.H. Daverveldt, and R. Kleiss, *Nucl. Phys.* B253, 441 (1985).
14. F.A. Berends and R. Kleiss, *Nucl. Phys.* B228, 537 (1983).
15. F.A. Berends and R. Kleiss, *Nucl. Phys.* B177, 237 (1981).
16. F. James and M. Roos, *Comp. Phys. Comm.* 10, 343 (1975).
17. K.G. Hayes and M.L. Perl, SLAC-PUB-4471, submitted to *Phys. Rev. D*.
18. R.E. Shrock, *Phys. Rev. D* 24, 1275 (1981).
19. B.F.L. Ward, *private communication*.
20. S. Weinberg, *Phys. Rev. Lett.* 18, 507 (1967).

21. T. Das, V.S. Mathur, and S. Okubo, *Phys. Rev. Lett.* 18, 761 (1967).
22. E. Braaten, *Phys. Rev. Lett.* 60, 1606 (1988).
23. E. Braaten, private communication.

TABLE I. τ branching fractions and normal errors assumed in the determination of the $e^+e^- \rightarrow \tau^+\tau^-$ background.

Decay mode	Branching fraction (%)
$\tau^- \rightarrow e^- \bar{\nu}_e \nu_\tau$	17.9 ± 0.4
$\tau^- \rightarrow \mu^- \bar{\nu}_\mu \nu_\tau$	17.6 ± 0.4
$\tau^- \rightarrow \pi^- \nu_\tau$	10.9 ± 0.6
$\tau^- \rightarrow (3\pi^\pm + \geq 0\pi^0)^- \nu_\tau$	13.4 ± 0.3
$\tau^- \rightarrow \rho^- \nu_\tau$	22.7 ± 1.0
$\tau^- \rightarrow (\pi^- + \geq 2\pi^0) \nu_\tau$	12.0 ± 2.0

TABLE II. Number of data events and expected backgrounds for $e\mu$ event subtypes with acolinearity angle $\theta_{acol} < 25^\circ$ and $\theta_{acol} > 25^\circ$.

	$e-\mu$ < 25°	$e-\mu$ > 25°
Data events	308	70
$e^+e^- \rightarrow \tau^+\tau^-$	294.7 ± 22.5	27.8 ± 5.9
$e^+e^- \rightarrow e^+e^-\mu^+\mu^-$	4.6 ± 2.6	16.7 ± 5.0
$e^+e^- \rightarrow e^+e^-\tau^+\tau^-$	9.8 ± 4.5	13.7 ± 5.9
$e^+e^- \rightarrow \mu^+\mu^-(\gamma)$	6.5 ± 3.2	0
Expected events	315.6 ± 23.3	58.2 ± 9.7
Excess events	-7.6 ± 23.3	11.8 ± 9.7

TABLE III. Number of data events and expected backgrounds for $e3$ and $\mu3$ event subtypes with $m_{inv} < 2.5 \text{ GeV}/c^2$ and $m_{inv} > 2.5 \text{ GeV}/c^2$.

	e vs 3 $m < 2.5$	e vs 3 $m > 2.5$	μ vs 3 $m < 2.5$	μ vs 3 $m > 2.5$
Data events	170	11	123	5
$e^+e^- \rightarrow \tau^+\tau^-$	153.4 ± 14.9	2.2 ± 1.6	108.1 ± 12.1	1.4 ± 1.3
$e^+e^- \rightarrow q\bar{q}$	0.5 ± 0.9	2.1 ± 1.8	0	0
$e^+e^- \rightarrow e^+e^-\tau^+\tau^-$	10.0 ± 4.2	1.7 ± 1.8	8.0 ± 3.9	0
$e^+e^- \rightarrow e^+e^-q\bar{q}$	3.2 ± 2.0	0.6 ± 0.8	0	0
$e^+e^- \rightarrow \mu^+\mu^-q\bar{q}$	0	0	1.0 ± 1.4	1.0 ± 1.4
Expected events	167.1 ± 15.6	6.6 ± 3.1	117.1 ± 12.8	2.4 ± 1.9
Excess events	2.9 ± 15.6	4.4 ± 3.1	5.9 ± 12.8	2.6 ± 1.9

TABLE IV. Number of data events and expected backgrounds for $e > 3$ and $\mu > 3$ event subtypes with $m_{inv} < 2.5 \text{ GeV}/c^2$ and $m_{inv} > 2.5 \text{ GeV}/c^2$.

	$e \text{ vs } > 3$ $m < 2.5$	$e \text{ vs } > 3$ $m > 2.5$	$\mu \text{ vs } > 3$ $m < 2.5$	$\mu \text{ vs } > 3$ $m > 2.5$
Data events	14	22	3	4
$e^+e^- \rightarrow \tau^+\tau^-$	2.3 ± 2.2	0.1 ± 0.3	2.0 ± 1.9	0.1 ± 0.3
$e^+e^- \rightarrow q\bar{q}$	0	2.0 ± 1.7	0	0
$e^+e^- \rightarrow e^+e^-\tau^+\tau^-$	0	0.5 ± 0.8	0	0
$e^+e^- \rightarrow e^+e^-q\bar{q}$	3.3 ± 2.0	10.9 ± 3.7	0	0
$e^+e^- \rightarrow \mu^+\mu^-q\bar{q}$	0	0	0	1.0 ± 1.4
Expected events	5.6 ± 3.0	13.5 ± 4.2	2.0 ± 1.9	1.1 ± 1.4
Excess events	8.4 ± 3.0	8.5 ± 4.2	1.0 ± 1.9	2.9 ± 1.4

TABLE V. Number of data events and expected backgrounds for $e\pi$ and $\mu\pi$ event subtypes with acolinearity angle $\theta_{acol} < 25^\circ$ and $\theta_{acol} > 25^\circ$.

	$e - \pi$ < 25°	$e - \pi$ > 25°	$\mu - \pi$ < 25°	$\mu - \pi$ > 25°
Data events	50	15	56	4
$e^+e^- \rightarrow \tau^+\tau^-$	58.5 ± 9.0	5.5 ± 2.5	54.5 ± 8.6	3.7 ± 2.0
$e^+e^- \rightarrow e^+e^-\tau^+\tau^-$	1.6 ± 1.6	11.2 ± 4.5	1.2 ± 1.3	2.1 ± 1.9
$e^+e^- \rightarrow e^+e^-q\bar{q}$	0	0.6 ± 0.9	0	0
$e^+e^- \rightarrow \mu^+\mu^-(\gamma)$	0	0	0	0.1 ± 0.3
$e^+e^- \rightarrow e^+e^-(\gamma)$	0.8 ± 1.2	0.8 ± 1.2	0	0
Expected events	60.9 ± 9.2	18.1 ± 5.4	55.7 ± 8.7	5.9 ± 2.8
Excess events	-10.9 ± 9.2	-3.1 ± 5.4	0.3 ± 8.7	-1.9 ± 2.8

TABLE VI. Number of data events and expected backgrounds for $e\pi(n\gamma)$ and $\mu\pi(n\gamma)$ event subtypes with acolinearity angle $\theta_{acol} < 25^\circ$ and $\theta_{acol} > 25^\circ$.

	$e - \pi(n\gamma)$ < 25°	$e - \pi(n\gamma)$ > 25°	$\mu - \pi(n\gamma)$ < 25°	$\mu - \pi(n\gamma)$ > 25°
Data events	215	28	162	17
$e^+e^- \rightarrow \tau^+\tau^-$	198.5 ± 21.9	11.9 ± 3.8	163.6 ± 19.0	6.5 ± 2.7
$e^+e^- \rightarrow q\bar{q}$	0	0.5 ± 0.9	0	0
$e^+e^- \rightarrow e^+e^-\tau^+\tau^-$	1.8 ± 1.8	9.6 ± 4.3	2.2 ± 1.9	5.2 ± 3.1
$e^+e^- \rightarrow e^+e^-q\bar{q}$	0.3 ± 0.6	0	0	0
$e^+e^- \rightarrow \mu^+\mu^-(\gamma)$	0	0	1.0 ± 1.2	0
$e^+e^- \rightarrow e^+e^-(\gamma)$	1.2 ± 1.6	2.3 ± 2.2	0	0
Expected events	201.8 ± 22.0	24.3 ± 6.2	166.8 ± 19.1	11.7 ± 4.1
Excess events	13.2 ± 22.0	3.7 ± 6.2	-4.8 ± 19.1	5.3 ± 4.1

TABLE VII. Numbers of SAT-tagged events and 'same-charge' events from data and Monte Carlo simulations for each event subtype.

	SAT-tagged events		Same-charge events	
	Data	Monte Carlo	Data	Monte Carlo
$e - \mu (< 25^\circ)$	2	2.6 ± 2.6	10	3.1 ± 2.6
$e - \mu (> 25^\circ)$	7	4.8 ± 3.6	9	11.6 ± 4.2
e vs 3 ($m < 2.5$)	5	3.0 ± 2.6	3	4.9 ± 2.3
e vs 3 ($m > 2.5$)	0	0	2	1.4 ± 1.2
μ vs 3 ($m < 2.5$)	4	0	2	2.0 ± 1.8
μ vs 3 ($m > 2.5$)	0	0	0	0
e vs > 3 ($m < 2.5$)	0	0		
e vs > 3 ($m > 2.5$)	1	0.7 ± 1.0		
μ vs > 3 ($m < 2.5$)	0	0		
μ vs > 3 ($m > 2.5$)	0	0		
$e - \pi (< 25^\circ)$	1	0.3 ± 0.7	0	0.2 ± 0.5
$e - \pi (> 25^\circ)$	1	3.0 ± 2.4	3	0.1 ± 0.3
$\mu - \pi (< 25^\circ)$	0	0	0	0.2 ± 0.5
$\mu - \pi (> 25^\circ)$	0	0	0	0
$e - \pi(n\gamma) (< 25^\circ)$	2	0	0	1.6 ± 1.3
$e - \pi(n\gamma) (> 25^\circ)$	5	1.4 ± 1.6	3	2.4 ± 2.1
$\mu - \pi(n\gamma) (< 25^\circ)$	0	0	2	0.8 ± 0.9
$\mu - \pi(n\gamma) (> 25^\circ)$	4	0.8 ± 1.1	0	0

TABLE VIII. Probability ratio R of data being consistent with background to data being consistent with background plus new lepton pair at (m_-, δ) . R is the product of the R_i for the 18 event subtypes.

(m_-, δ) (GeV/ c^2)	R
(0.3,0.3)	9.2×10^{-1}
(0.5,0.5)	3.7×10^2
(0.7,0.7)	2.4×10^{15}
(1.8,1.8)	1.6×10^{48}
(2.0,0.5)	1.9×10^{22}
(2.0,1.0)	2.5×10^{35}
(2.5,2.5)	2.7×10^{38}
(3.0,0.3)	1.5×10^2
(3.0,1.8)	1.0×10^{32}
(4.0,0.5)	4.3×10^{12}
(4.0,1.0)	1.7×10^{22}
(4.0,4.0)	8.8×10^{49}
(5.0,2.5)	7.3×10^{42}
(6.0,0.3)	2.1×10^0
(6.0,1.8)	1.3×10^{22}
(7.0,0.7)	2.0×10^7
(7.0,7.0)	1.6×10^{41}
(8.0,0.5)	1.5×10^2
(9.0,4.0)	5.6×10^{28}
(10.0,1.0)	1.3×10^3
(10.0,1.8)	3.9×10^{11}
(10.0,2.5)	1.3×10^{16}
(10.0,10.0)	1.9×10^{24}
(12.0,1.8)	2.0×10^5
(12.0,7.0)	2.6×10^{14}
(13.0,0.7)	1.0×10^0
(13.0,1.8)	1.6×10^3
(13.0,2.5)	2.2×10^5
(13.0,4.0)	3.2×10^9
(14.0,1.0)	1.2×10^0
(14.0,7.0)	2.2×10^0
(14.0,10.0)	5.6×10^1
(14.0,14.0)	2.5×10^0

TABLE IX. Best fit τ branching fractions from this analysis assuming absence of new lepton pairs with $m_- < 14.5 \text{ GeV}/c^2$.

Decay mode	Branching fraction (%)
$\tau^- \rightarrow e^- \bar{\nu}_e \nu_\tau$	17.8 ± 1.0
$\tau^- \rightarrow \mu^- \bar{\nu}_\mu \nu_\tau$	17.5 ± 1.0
$\tau^- \rightarrow \pi^- \nu_\tau$	9.8 ± 1.2
$\tau^- \rightarrow (3\pi^\pm + \geq 0\pi^0)^- \nu_\tau$	13.9 ± 1.1
$\tau^- \rightarrow (\pi^- + \geq 1\pi^0) \nu_\tau$	36.0 ± 2.6

FIGURE CAPTIONS

FIG. 1. Dependence of L^- -branching fractions on δ for (a) $m_- = 2 \text{ GeV}/c^2$ and (b) $m_- = 10 \text{ GeV}/c^2$. Decay modes are (1) $L^- \rightarrow L^0 e^- \bar{\nu}_e$, (2) $L^- \rightarrow L^0 \mu^- \bar{\nu}_\mu$, (3) $L^- \rightarrow L^0 \pi^-$, (4) $L^- \rightarrow L^0 \rho^-$, (5) $L^- \rightarrow L^0 K^-$, (6) $L^- \rightarrow L^0 K^{*-}$, (7) $L^- \rightarrow L^0 a_1^-$, (8) $L^- \rightarrow L^0 \bar{u}d$, (9) $L^- \rightarrow L^0 \bar{c}s$, and (10) $L^- \rightarrow L^0 \tau^- \bar{\nu}_\tau$.

FIG. 2. Visible energy spectrum, neglecting detector acceptance effects, from $L^- \rightarrow L^0 + \text{multihadrons}$ when $E_{beam} = 14.5 \text{ GeV}$ and $m_- = 10 \text{ GeV}/c^2$.

FIG. 3. New lepton pairs are excluded, with $R > 9$, from the hatched regions by the $e\mu$ event subtypes.

FIG. 4. New lepton pairs are excluded, with $R > 9$, from the hatched regions by the $e3$, $\mu3$, $e > 3$, and $\mu > 3$ event subtypes.

FIG. 5. New lepton pairs are excluded, with $R > 9$, from the hatched regions by the $e\pi$, $\mu\pi$, $e\pi(n\gamma)$, and $\mu\pi(n\gamma)$ event subtypes.

FIG. 6. New lepton pairs are excluded from the hatched regions by all event subtypes combined. The excluded regions are shown in (a) for $R > 9$ with a linear δ scale and in (b) for $R > 9$ (above lower contour) and $R > 99$ (above upper contour) with a logarithmic δ scale.

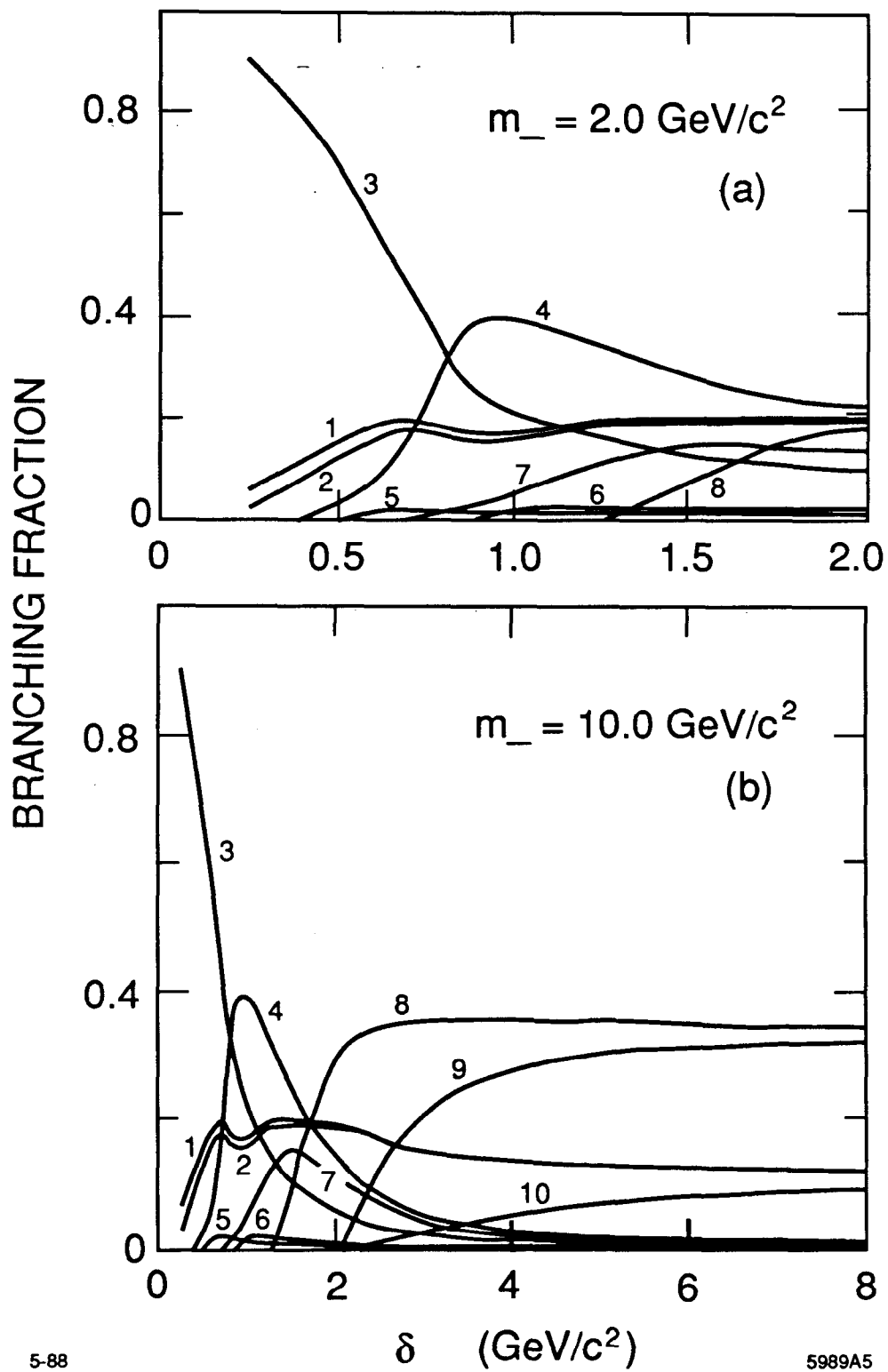


Fig. 1

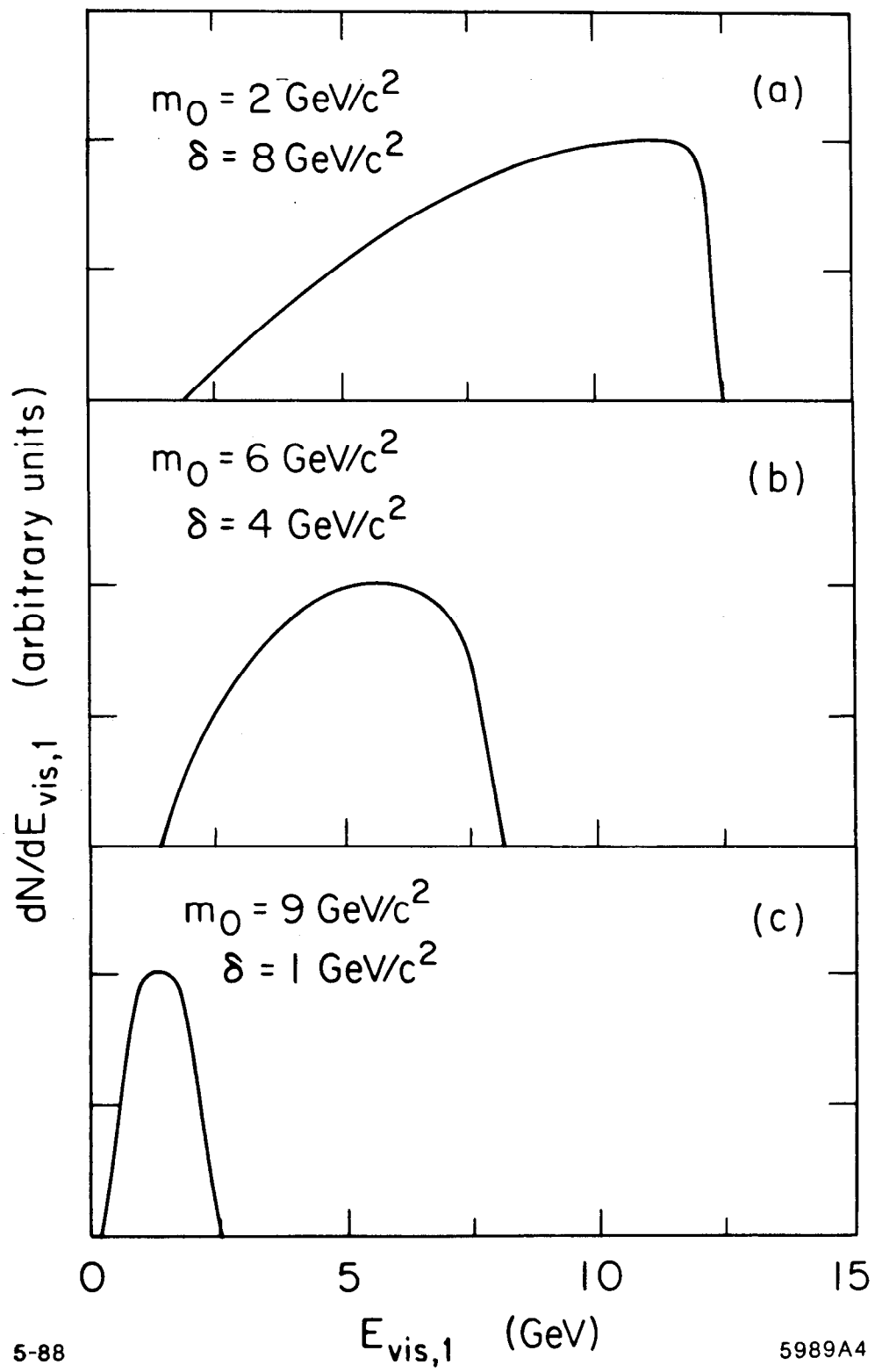


Fig. 2

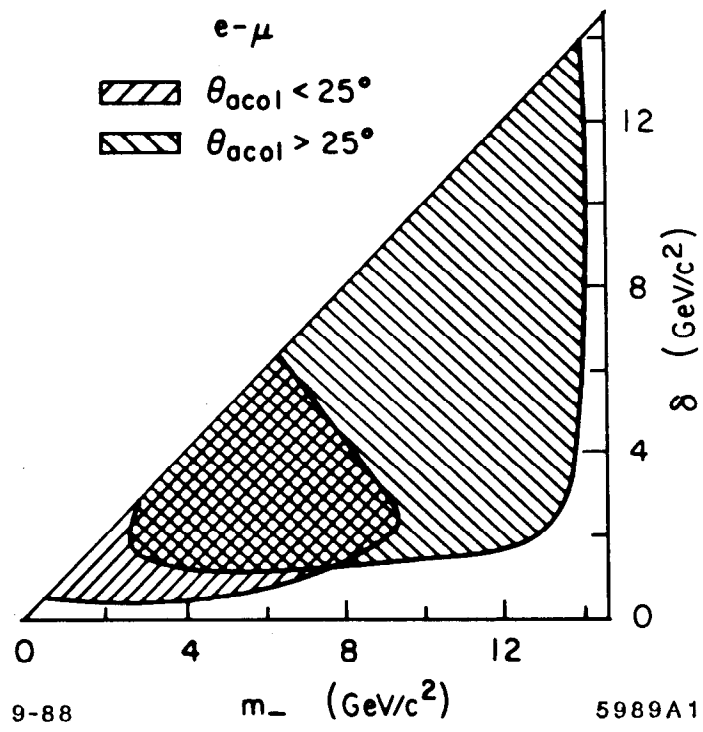




Fig. 3

 $m_{inv} < 2.5 \text{ GeV}/c^2$
 $m_{inv} > 2.5 \text{ GeV}/c^2$

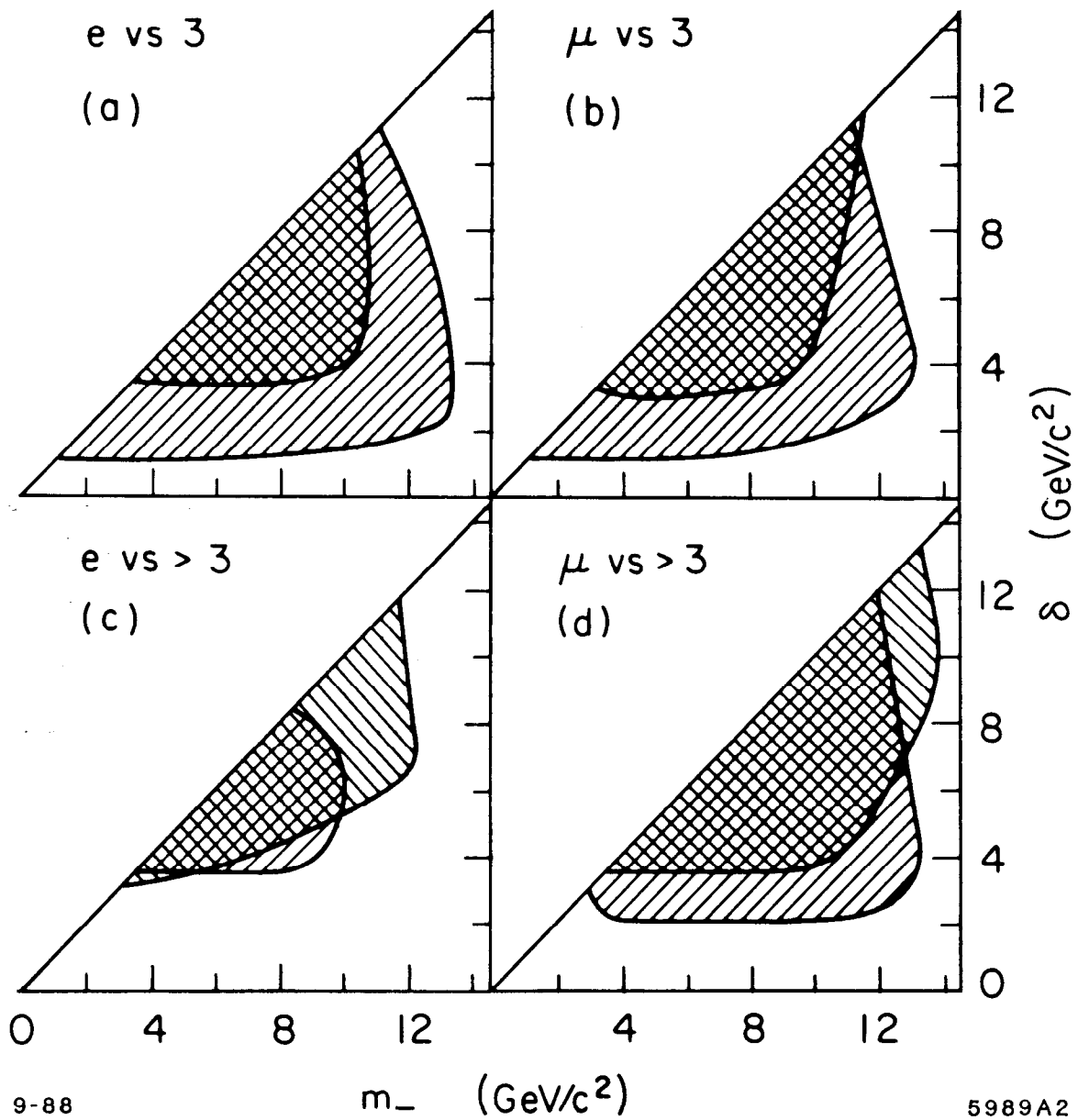


Fig. 4

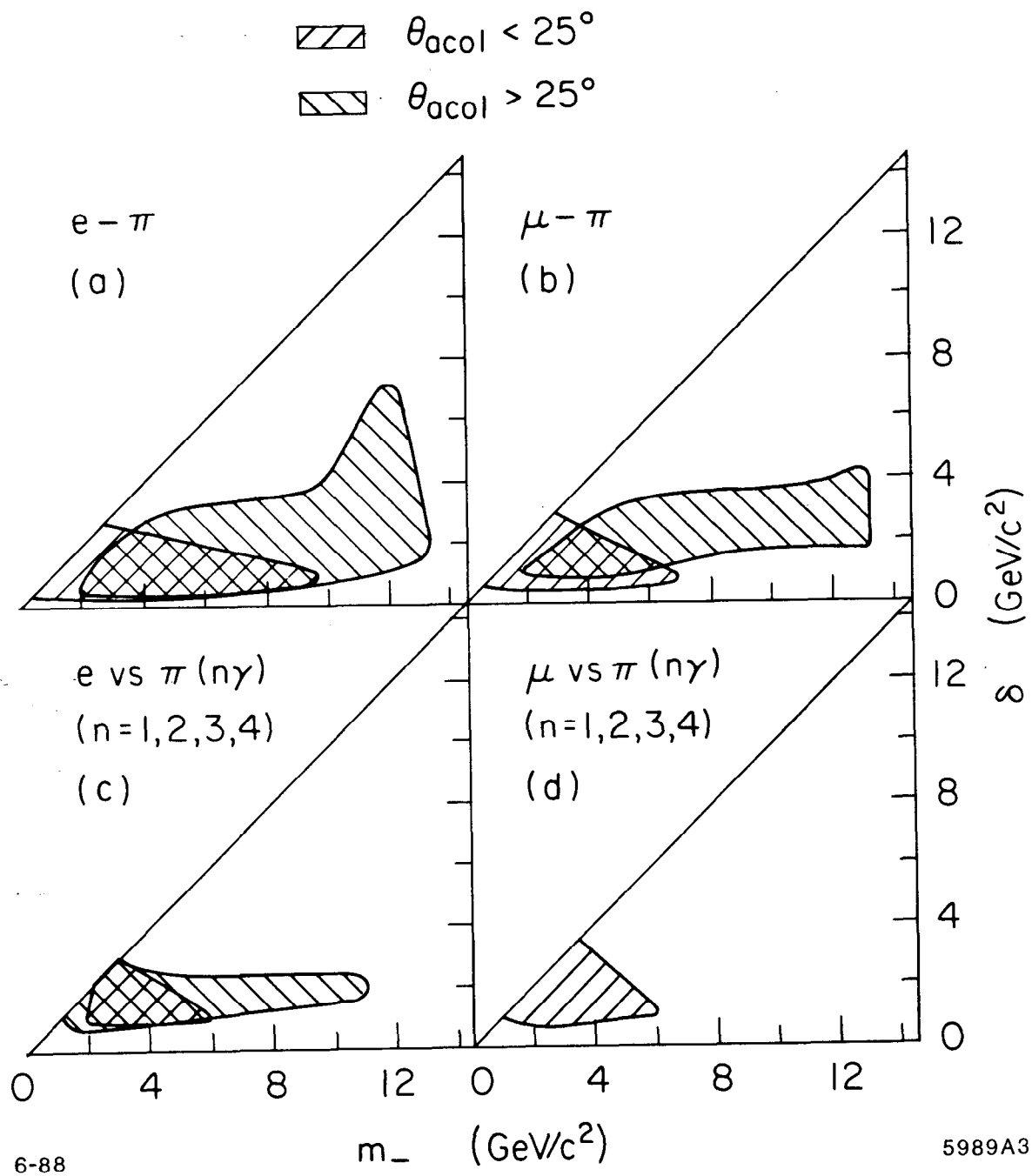


Fig. 5

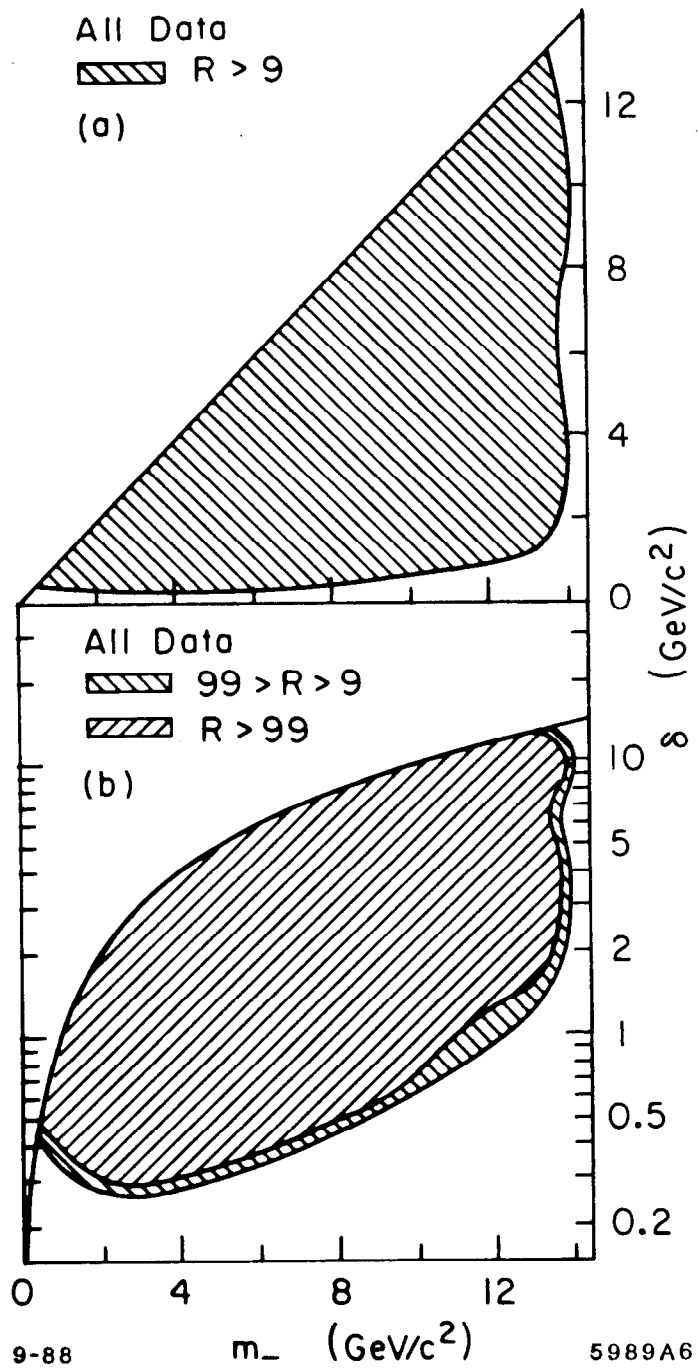


Fig. 6